Injected-Ion Mobility Analysis of Biomolecules

Yansheng Liu
Stephen J. Valentine
Anne E. Counterman
Cherokee S. Hoaglund
David E. Clemmer
Indiana University

Injected-ion mobility techniques combined with MS can provide information about the three-dimensional structures of ions. Recently, electrospray ionization (ESI) (*1*) and matrix-assisted laser desorption ionization (MALDI) (*2*) sources have been coupled with injected-ion mobility methods to investigate the conformations of solvent-free biomolecules in the gas phase (*3–5*).

This Report describes biomolecular structural studies using the injected-ion mobility/MS approach. Several examples will illustrate how these methods can be used to resolve and characterize conformations, examine the dynamics of protein unfolding and folding in the gas phase, and complement MS methods for characterizing oligosaccharide isomers. [The development and application of these methods has been reviewed elsewhere (*6*).]

Ion mobility spectrometry is a well-established analytical technique for detecting and identifying analytes based on their mobilities through inert buffer gases (*7*). Combining ion mobility data with detailed mobility calculations (*8, 9*) has created an integrated approach that can provide information about the three-dimensional geometries of ions in the gas phase. In some systems, remarkably detailed geometries can be gleaned (*10, 11*).

Injected-ion mobility can be used to characterize conformations, examine protein folding, and complement MS methods.

ESI and MALDI sources for MS have opened new doors for the exploration of biomolecular structure. Biomolecular conformations can now be examined in vacuo, making it possible to begin understanding the nature of conformations that arise solely from intramolecular interactions.

The available methods for studying gas-phase conformation cannot provide atomically detailed information. However, many of the qualitative behaviors of biomolecules in solution—such as folding and unfolding—have been observed in the gas phase. Injected-ion mobility methods provide a versatile means of characterizing the structures of these ions because both physical and chemical approaches to structural analysis can be used.

For example, by varying the kinetic energy used to inject ions into the inert buffer gas, it is possible to induce structural transitions that appear to correspond to biomolecular unfolding and folding events (*12–15*). At high injection energies, the ions dissociate and sequence information can be obtained (*16*). In the chemical approach, the buffer gas is doped with a reagent and it is possible to examine the chemistry that occurs on the surfaces of conformers having different shapes. Shape-specific hydrogen/deuterium (H/D) exchange (*13*), solvent adsorption (*17*), and proton transfer reactions (*18*) have also recently been reported. [Other methods being developed to examine gas-phase protein conformations include ion scattering with triple quadrupole instruments (*19–21*), H/D exchange (*22–24*), proton-transfer reactivity studies (*25, 26*), and microscopy studies of the hillocks formed upon bombardment of surfaces with high-energy protein ions (*27*).]

Experimental approach

When a pulse of biological ions is injected into a static buffer gas and subjected to a weak electric field, different charge states and conformations are separated because of differences in their mobilities through the gas. The method has some similarities with electrophoresis techniques; thus, it can be thought of as gas-phase electrophoresis.

The ions' drift velocities v_D are given by $v_D = KE$, in which E is the electric field strength and K is the mobility constant. The mobility is proportional to the charge state of the ion. Within a given charge state, ions with compact conformations have higher mobilities than more diffuse ones.

S0003-2700(97)09051-3 CCC: $14.00

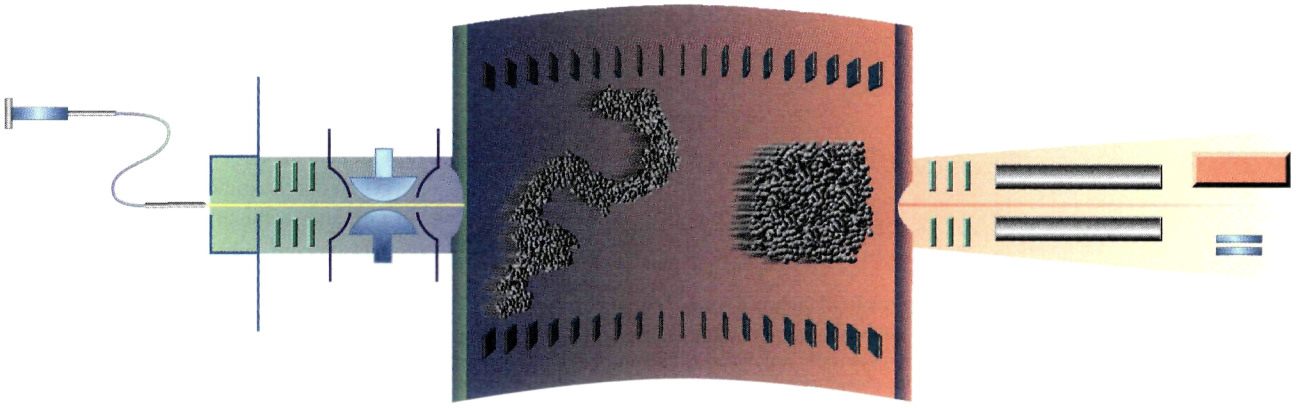

CESAR CAMINERO/FOCALPOINT

Figure 1 shows a schematic of our experimental apparatus. Biological ions are electrosprayed into a variable-temperature differentially pumped drying region, extracted into a vacuum chamber, and focused into an ion beam. An electrostatic gate is used to inject a short pulse of ions through a small aperture into a drift tube containing a buffer gas. Recently, we coupled a quadrupole ion trap storage device to the front of the drift tube, as shown in Figure 1 (*28*). (The data in this Report were recorded before addition of the ion trap, which offers several advantages outlined later.) Ions travel through the buffer gas under the influence of a weak, uniform electric field provided by an ion lens system. Ions that exit the drift tube are focused into a quadrupole mass filter that allows selection of individual m/z species, which are detected by an off-axis collision dynode/microchannel plate detector.

An example of ion mobility distribution for the +8 state of cytochrome *c* is also shown in Figure 1. Three peaks are clearly resolved, indicating that at least three conformations having identical m/z ratios are present. For the purpose of comparison, it is useful to convert the data into a reduced mobility, which depends only on the intrinsic properties of the ion and buffer gas.

The reduced mobility is given by (*29*)

$$K_O = \frac{L}{t_D E}\frac{P}{760}\frac{273.2}{T} \qquad (1)$$

in which t_D is the measured drift time, E is the electric field, L is the length of the drift tube, P is the buffer gas pressure (in Torr), and T is the buffer gas temperature. For characterizing conformations, it is useful to convert the data to collision cross sections σ. These cross sections are derived directly from the experimental data using (*29*)

$$\sigma = \frac{(18\pi)^{1/2}}{16}\frac{ze}{(k_B T)^{1/2}}\left[\frac{1}{m_I}+\frac{1}{m_B}\right]^{1/2} \frac{t_D E}{L}\frac{760}{P}\frac{T}{273.2}\frac{1}{N} \qquad (2)$$

which contains the reduced mobility, and in which z is the charge state, e is the charge of an electron, k_B is Boltzmann's constant, N is the neutral number density, and m_I and m_B are the masses of the ion and buffer gas, respectively. Parameters E, L, P, T, and t_D can be precisely measured. Thus, the reproducibility of measured mobilities or cross sections is excellent, with different measurements usually agreeing to within 1%.

Obtaining structural information

Calculating collision cross sections. Information about the structures of different ions is obtained by comparing the experimental cross sections with values that are calculated for trial conformations. By assuming hard-sphere collisions, the collision cross section of a large ion with inert gases can be estimated by considering only the sizes and orientations of the colliding partners. In the weak electric field used for the mobility measurement, ions do not appear to align. Therefore, calculations of cross sections for trial conformations must consider all possible orientations of the colliding partners. This calculation is accomplished by determining an orientationally averaged projection of the molecule.

An example drift time that has been derived from the calculated projections of the crystal coordinates of cytochrome *c* is shown in Figure 1. The calculated drift time is slightly shorter than the first peak observed experimentally. Thus, ions that arrive near the calculated value must have highly compact conformations. However,

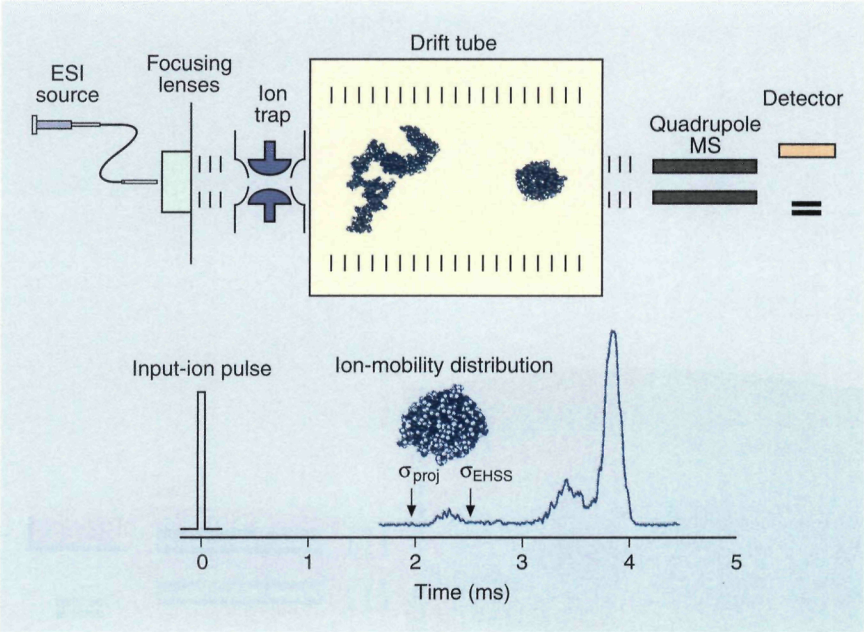

Figure 1. Diagram of an injected-ion mobility/mass spectrometer.

Instrument uses a continuous ESI source and an ion trap for ion accumulation and pulsing. Mass selection occurs via a quadrupole mass spectrometer after ions have exited the drift tube. Also shown is an ion mobility distribution recorded for the +8 state of cytochrome *c*. The arrows show drift times derived from cross sections that were calculated by two methods for the crystal structure coordinates for cytochrome *c*.

they are not necessarily the same structure as that found in the solution or in the crystal. Peaks that are observed at longer times must correspond to ions that have substantially more open (or diffuse) conformations. The projection approximation method has merit because it is simple and appears to provide accurate assignments for many different types of geometries found for atomic clusters (*6*). However, the analysis ignores all of the interactions associated with the collision and does not address issues associated with changes in conformation that may occur over the millisecond timescale of the experiment.

Calculations of collision cross sections with more realistic potentials and which account for the dynamic nature of the biomolecule are being attempted (*30, 31*). Currently, it appears that the projection approximation gives a lower limit to the true cross section and, for nearly all geometries, gives results that are within 20% of cross sections calculated by more rigorous approaches. For most geometries, the agreement is much better.

Shvartsburg and Jarrold recently developed an exact hard sphere scattering (EHSS) method (generating values best viewed as upper limits) that accounts for the scattering of the buffer gas (*32*). With this method, the calculated drift time for the crystal coordinates (σ_{EHSS} in Figure 1) is slightly greater than the drift time for the first experimental peak (Figure 1).

Generating trial conformations with molecular modeling methods. A limitation in assessing the accuracy of any method that calculates cross sections for large biomolecules is the absence of a calibration standard. In the cluster systems, calculated mobilities for well-established coordinates of C_{60}^+ were in close agreement with experimental values, providing convincing evidence that rather detailed structural information is obtainable (*6*). This allowed more speculative trial structures to be tested, which were either rejected because they did not fit the data or accepted as possible structures.

That any biomolecular structure known to exist in solution will be retained in the gas phase is not guaranteed. It has been postulated that in the apolar vacuum environment biomolecules may effectively turn inside out (*33*). Thus, although assessing the relative degree of "compactness" or "elongation" of eight different conformations is possible, assignment of the conformational details—such as which residues are on the surface—is not possible from this analysis alone.

An advantage for studying biomolecular systems is the commercially available, sophisticated molecular modeling software for generating conformations. Many of these programs allow calculations of in vacuo conformations. For small biomolecules such as peptides, short DNAs, and oligosaccharides (containing ~20 residues), it is possible to generate thousands of trial energy-minimized conformers and calculate collision cross sections for these. Bowers and co-workers adopted this method for studies of bradykinin and have attempted to extract some of the structural details (*3, 4*).

With so little known about in vacuo conformations, the interplay between the ion mobility data and molecular modeling results is important. Ion mobility results for rigid molecules with known structures are useful in determining accurate force fields for molecular modeling calculations. Experimental mobilities for biomolecules are benchmarks for modeling. The conformational details of in vacuo structures hinge on the reliability of the modeling results. As mentioned later, the ability of ion mobility methods to resolve different conformers is rapidly improving. The development of accurate methods for calculating cross sections and better force fields for generating trial conformations are key elements in the future progress of this field.

Instrument performance

Resolving power. The resolving power $t_D/\Delta t$ (in which Δt is the full width at half maximum of the ion mobility peak) for ions varying in shape and charge state is given by (*34*)

$$\frac{t_D}{\Delta t} = \left[\frac{LEze}{16k_B T \ln 2}\right]^{1/2} \qquad (3)$$

Although a term representing the buffer gas pressure does not appear in this expression, the buffer gas plays a key role in the resolving power. To inject ions into the drift tube, the ion's momentum must exceed the flow of buffer gas that leaks out the drift tube entrance. For biomolecular ions with large collision cross sections, a practical limit for the buffer gas pressure is ~10 Torr. At higher pressures, excessively high injection energies

(which induce structural changes or fragmentation as discussed later) are required to introduce ions into the drift tube. The ~10 Torr pressure limit restricts the values for E and L, because of the electrical breakdown of the gas, and also restricts the instrument's size.

The drift tube in our present injected-ion instrument is 32.4-cm long and is typically operated using drift fields of ~15 Vcm^{-1} with He, ~30 Vcm^{-1} with Ar, or ~50 Vcm^{-1} with N_2. For singly charged ions at room temperature, this arrangement provides resolving powers ranging from ~20 to 60. An additional twofold improvement in resolution is obtained by cooling the buffer gas to near-liquid nitrogen temperatures. We have measured resolving powers in low-temperature nitrogen buffer gas in excess of 100. The resolution increases linearly with the square of the charge state, as expected from eq 2. Thus, for multiply charged biological ions, attaining resolving powers of several hundred, approaching the mass-to-charge based separation capabilities of low-end linear time-of-flight mass spectrometers, should be possible.

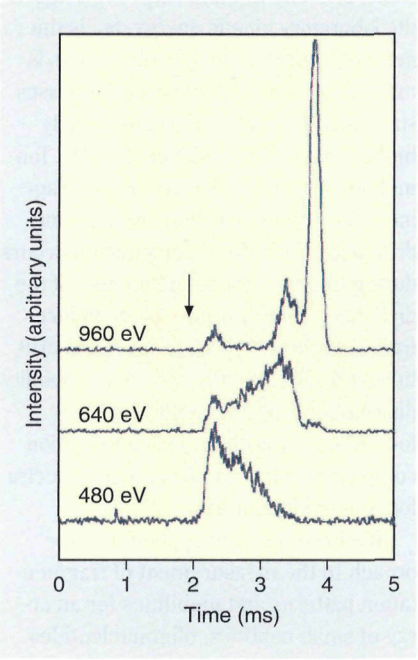

Figure 2. Ion mobility distributions for the +8 charge state of cytochrome c.

A 8×10^{-5} M protein solution in 49:49:2 water: acetonitrile:acetic acid is electrosprayed into the instrument; spectra are recorded at injection energies of 480, 640, and 960 eV. Arrow corresponds to the calculated drift time for the crystal structure of cytochrome *c* using the projection approximation.

By coupling high-pressure ion sources directly to high-pressure drift tube instruments that operate at pressures of 10^2 to 10^3 Torr, it is possible to substantially increase the drift field and resolution (*6*, *35*). This approach provides high selectivity for analytical ion mobility spectrometers. At high pressures, ions cannot be injected into the drift tube. Therefore, it is not possible to take advantage of collisional activation processes (which are accessible in the low-pressure injected-ion mode). Nevertheless, the higher resolving powers are a clear advantage.

Duty cycle. Pulsed ionization sources, such as MALDI, are naturally suited for ion mobility studies because the experiment can be initiated with the laser pulse and all of the ions that are formed can be used for experiments. Bowers and co-workers have used this advantage in their MALDI studies of bradykinin (*3*, *4*). However, for continuous ion sources such as ESI, pulsing significantly reduces the duty cycle of the experiment.

For the experimental data in this Report, ion pulses of 25 to 50 μs were used and ion mobility distributions were recorded for 5 to 10 ms between pulses. These conditions provide a duty cycle of only 0.25 to 1.0% and, with these low signals, acquiring data for minutes to several hours is sometimes necessary.

To address this problem, we have recently coupled an ion trap to the entrance of our drift tube (Figure 1) (*28*). The ion trap consists of two endcaps and a center ring, which introduce 1-μs pulses of ions into the drift tube and then accumulates ions from the ESI source while recording the ion mobility spectrum. This method concentrates the continuous beam of ions between pulses and is similar to an approach used by Lubman and co-workers to increase ESI signals in time-of-flight MS experiments (*36*).

Our initial studies show that for some ions input pulses can be reduced to 1 μs, while the ion signal per pulse is increased by factors of ~10 to 30 (*28*). Pulse frequencies can also be reduced without a significant signal loss. With these improvements, we have reduced the time required to acquire an ion mobility distribution for cyclodextrin from several minutes to <10 s. This corresponds to a total sample consumption of only 20 pmols and demonstrates the feasibility of making rapid, sensitive measurements. It is also possible to record mobilities for fragment ions formed during collision-induced dissociation, which should greatly improve the ion mobility method as a means of qualitatively analyzing biological samples.

Collision-induced structural transitions

As ions enter the drift tube, they are rapidly heated as their kinetic energies are thermalized by collisions with the buffer gas. Further collisions cool the ions to the buffer gas temperature. This heating/cooling cycle induces structural transformations. In some cases, the heating/cooling process anneals unstable conformations formed during the electrospray process into more stable ones (*14*). However, recent work has shown that metastable conformations, which do not refold on the timescales of these experiments, are also formed (*15*).

Figure 2 shows ion mobility distributions measured as a function of injection energy for the +8 charge state of cytochrome *c* (*13*). At low injection energies (200 to 500 eV), the ion mobility distribution is dominated by a distribution of compact conformations that have drift times of ~2.2 to 3.0 ms. The 2.2-ms drift times are near the values calculated for the native conformation from the projection model. However, this feature is too broad to be due to a single conformation and, thus, must be caused by several conformations with similar cross sections.

When the injection energy is increased (~600 to 750 eV), the feature corresponding to compact forms of the protein begins to disappear and a broad feature with a maximum near 3.2 ms is observed. A small shoulder, at times longer than 3.6 ms, is also observed. At higher injection energies (~950 to 2000 eV), the ion mobility distributions are dominated by a peak that arrives at ~3.8 ms. The long drift time observed for this ion indicates that it has an extremely open conformation. No dissociation is observed under the conditions of these experiments; thus the changes observed are

due to changes in the protein conformation. In this case, the protein has undergone an unfolding transition.

It appears that during the electrospray process a relatively compact conformation is formed. As the ions are injected into the drift tube, they anneal into a more stable elongated gas-phase conformation. To minimize the heating/cooling cycle as ions are injected into the drift tube and to observe conformations that are closely related to those formed by ESI, the lowest possible injection energies should be used.

The driving force for a structural transition involving unfolding of a multiply charged ion is the relief of coulombic repulsion energy. In the absence of solvent, which has a high dielectric constant (~80 for water), coulombic repulsion is reduced by unfolding to form an open conformation. Consistent with the +8 injection energy data are ion mobility distributions and cross sections measured for other protonation states. Lower protonation states favor more compact conformations, while higher states favor open structures (*12, 19–21, 27*).

The details of the open and compact conformations are still under investigation, and several models have emerged. Gas-phase hydrogen bonding should favor α-helical and β-sheet conformations and help stabilize compact conformations (*12*). Intramolecular charge-solvation is also expected to play an important role in lowering the coulombic repulsion energy (*12, 25, 26*).

To test the latter idea, we have recently measured the collision cross sections for negatively charged (deprotonated) cytochrome *c*. Deprotonation should occur at the 11 acidic aspartic and glutamic acid sites, while protonation should occur at the 22 basic arginine, lysine, and histidine residues. The cross sections derived from the largest feature observed in the ion mobility distributions for deprotonated cytochrome *c* are similar to those observed for the protonated ions for high charge states (±10 to 12 H) and low charge states (±4 or 5 H).

The similarity in cross sections for these charge states can be understood by considering which forces are dominant. For low charge states, with low coulombic repulsion energies, hydrogen bonding and van der Waals interactions dominate, favoring compact conformers. Alternatively, for high charge states with large coulombic repulsion energies, extended conformations are favored.

For intermediate states (7 to 9) of protonated and deprotonated ions (where repulsive coulombic destabilizing forces and attractive bonding forces are similar), different collision cross sections are observed for the protonated and deprotonated systems of the same charge state. Here, the charge type appears to influence the conformation. This result can be understood by noting that the local environments surrounding acidic and basic residues are different. Thus, the ability to stabilize protonated or deprotonated forms varies near the point where the attractive and repulsive forces are comparable.

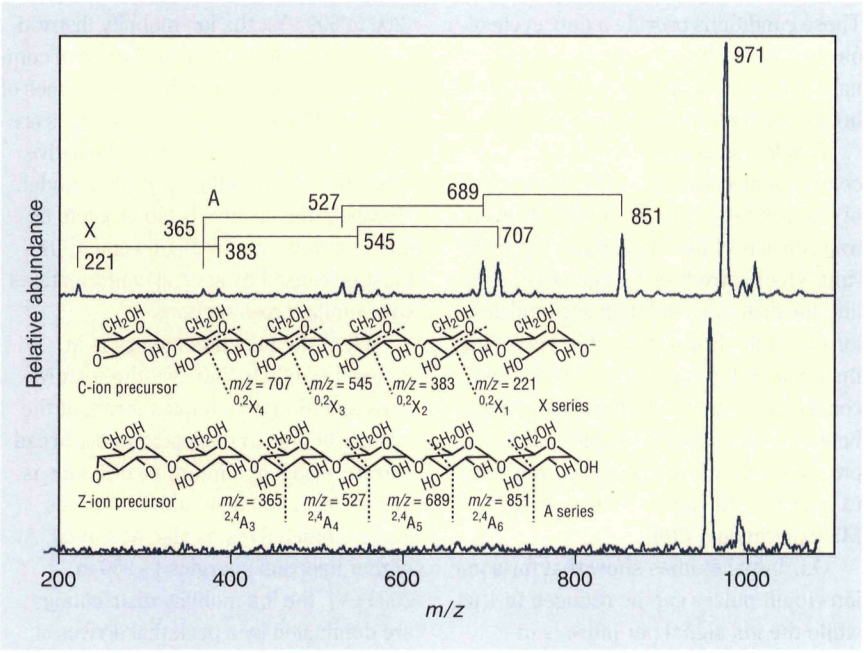

Figure 3. Negative-ion mass spectra for α-cyclodextrin.

Sample injected into ~3 Torr of nitrogen buffer gas using injection energies of (bottom) 400 and (top) 1000 eV. Inset shows C- and Z-ion precursors that are expected to yield X- and A-series fragments. Reported *m/z* ratios correspond to the positions of peak centers and have uncertainties of less than ±1 amu.

Collision-induced dissociation

At high injection energies, the transient heating/cooling cycle that occurs as ions are injected into the drift tube can be used to induce fragmentation. The degree of fragmentation can be controlled by varying the injection energy and the drift tube buffer gas. The latter effect is caused by differences in center-of-mass-collision energy E_{com} of the initial ion-buffer gas collisions, given by $E_{lab}(m_B/m_I + m_B)$: E_{lab} is the laboratory kinetic energy, m_B is the mass of a buffer gas molecule, and m_I is mass of the ion. High-mass buffer gasses such as N_2 and Ar lead to substantially higher levels of dissociation than He. Ion mobility distributions recorded for fragments at varying injection energies and drift fields show that fragmentation occurs during the first several millimeters of the drift tube. Thus, it is possible to induce fragmentation at the entrance of the drift tube and subsequently record ion mobility distributions for fragments that were formed upon injection. This information complements fragmentation mass spectra for isomer identification.

We have recently applied this approach to the measurement of fragmentation patterns and mobilities for an array of small peptides, oligonucleotides, oligosaccharides, and the fragments of these ions. Some of these systems display sequence-dependent fragmentation patterns, making the approach a viable strategy for sequencing small biopolymers. Application of these methods to oligosaccharides is especially interesting. Unlike the linear covalent se-

quences of peptides and nucleic acids, oligosaccharides exist in a multitude of isomeric forms because of different branching patterns, sugar-ring structures, and anomeric configurations. Analysis of these species with MS methods alone is inadequate for complete structural determination because different structural isomers have identical *m/z* values.

Figure 3 shows example mass spectra recorded for negatively charged (deprotonated) α-cyclodextrin (CD), a six-residue cyclic sugar that was recorded by using nitrogen as the buffer gas (*16*). At an injection energy of 400 eV, the deprotonated parent ion dominates the mass spectrum. As the injection energy is increased to 1000 eV, a series of fragment ions is observed. The fragmentation pattern is consistent with a series of cross-ring cleavages of the precursor ions shown in Figure 1. The related β- and γ-CD sugars—analogous cyclic sugars containing seven and eight residues, respectively—display similar fragmentation patterns.

Ion mobility distributions for several of the fragment ions of α-cyclodextrin are shown in Figure 4a. As the fragment size decreases, the mobility increases, a result of the decreasing size of the lower *m/z* fragments. The *m/z* = 545 fragment ion displays a broad peak that can be resolved into three distinct ion types. This indicates that either multiple isomers or conformers are formed for this fragment.

Figure 4b shows ion mobility distributions recorded for *m/z* = 707 fragment ions formed from the dissociation of α-, β-, and γ-cyclodextrin. The *m/z* = 707 fragments from the different precursors have mobilities that are identical within 0.5%, which is within our experimental uncertainty. This outcome is consistent with the formation of identical isomer fragments, as is expected for sugars with closely related structures. Additionally, there is no evidence for variations between conformations of ions that are formed from different precursor ions.

Figure 4c shows ion mobility distributions recorded for several isomers that can be distinguished based on their ion mobility distributions. Melezitose [α-D-Glcp(1-3)-β-D-Fruf-(2↔1)-α-D-Glcp] and raffinose [α-D-Galp-(1→6)-α-D-Glcp-(1↔2)-β-D-Fruf] are each three-residue

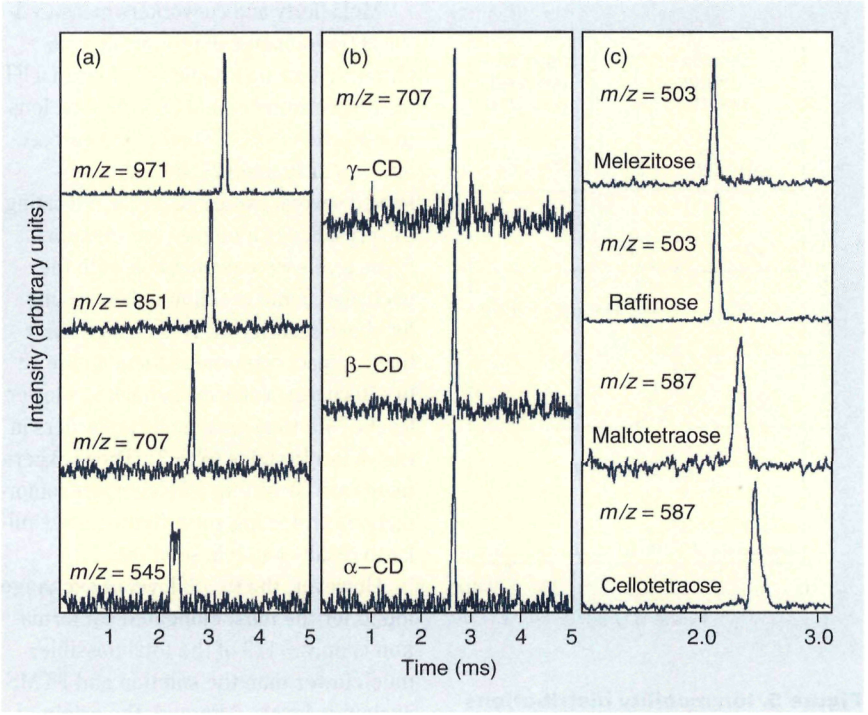

Figure 4. Ion mobility distributions for cyclodextrins and fragments formed by collision-induced dissociation.

(a) Ion mobility distributions for α-cyclodextrin and several fragments in nitrogen buffer gas (1000-V injection voltage). (b) Ion mobility distributions for the *m/z* = 707 fragment formed by collision-induced dissociation of α-, β-, and γ-cyclodextrins. (c) Ion mobility distributions for sugars: top two distributions are for melezitose and raffinose parent (*m/z* = 503) ions; bottom two are for *m/z* = 587 fragments of maltotetraose and cellotetraose. All distributions were recorded using nitrogen buffer gas; data are normalized to a pressure of 2.9 Torr.

sugars that differ in sequence, linkage, and anomeric configuration. Negative-ion ESI of both sugars generates a parent *m/z* = 503 ion, and the mobilities for these vary by 1.3%, making it possible to barely distinguish between them based on their mobilities.

Maltotetraose and cellotetraose are each four-residue sugars that differ only in the glycosidic linkage (α-D and β-D, respectively). The fragmentation patterns of the parent ions are virtually identical, making it impossible to distinguish between them based on MS methods alone. However, the parents and fragments that are observed have different mobilities. An example is shown for the *m/z* = 587 ion (Figure 4c). In this case, the mobility difference is almost certainly attributable to differences in conformations that arise from the nature of the glycosidic linkage. Maltotetraose with α-D linkages is relatively free to adopt compact conformations; steric factors for the β-D bonded cellotetraose cause more extended structures to be favored.

Chemical reactivity of gas-phase conformations

The chemistry that occurs on the surfaces of shape-resolved conformations may be monitored by doping the drift tube buffer gas with low concentrations of reagents. Jarrold and co-workers, using this approach to study the binding of the first few waters to different conformations, found evidence that some of these water molecules are critical in establishing the conformations of biomolecules.

We are investigating a combined ion mobility and chemical reactivity approach for simultaneously characterizing the overall shape and surface of different conformations. The number of hydrogens that can undergo rapid H/D exchange for specific conformation types may be monitored by adding a small fraction of deuterated solvents, such as D_2O, to the buffer gas. The basic idea is that hydrogens bound to heteroatoms at the surface of the biomolecule should be accessible for exchange with the deuterated solvent, whereas those that reside within the bio-

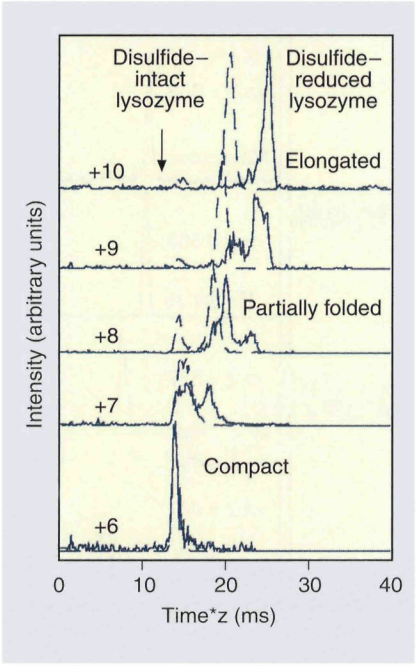

Figure 5. Ion mobility distributions recorded using He buffer gas for disulfide-intact (dashed lines) and disulfide-reduced (solid lines) lysozyme.

Data are shown on a modified-time axis (drift time multiplied by the charge state), which normalizes for differences in the effective field. Data are also normalized to a pressure of 2.000 Torr. Arrows show calculated drift times for the crystal conformation and an extended linear conformation.

molecule will be protected and will undergo much slower exchange. Other factors may also influence exchange.

In these studies, the conformation type is generated by controlling the injection energy, as shown in Figure 2. The maximum number of rapidly exchanging hydrogens is found by varying the deuterated solvent pressure and drift voltage (which varies the amount of time that the ions are exposed to the solvent) and determining the maximum increase in m/z of the parent ion after solvent exposure.

We have used this method to measure the maximum number of rapidly exchanging hydrogens and kinetics of H/D exchange for the compact and elongated conformations of horse-heart cytochrome *c*, which has 198 exchangeable hydrogens. In neutral solution, NMR data have shown that 144 of these hydrogens undergo rapid exchange, although the remaining hydrogens are largely protected along α-helical regions.

McLafferty and co-workers measured the H/D exchange of protonated cytochrome *c* ions by trapping the ions in a FT mass spectrometer and exposing the ions to low levels (~10^{-7} Torr) of D_2O for seconds up to 30 min (*23, 24*). They observed several exchange levels, indicating the presence of multiple conformations. Some levels were comparable with the exchange found in solution. Our results for shape-resolved H/D exchange show that compact conformers found in the +8 to +10 charge states exchanged at a lower level (~45) than elongated conformers in the +8 to +18 states (62 ± 3). These experiments are consistent with compact conformations protecting some hydrogens, similar to results found in solution.

However, the 62 ± 3 level of exchange found for the most elongated conformation is only ~1/3 of the total possible, much lower than the solution and FTMS exchange levels. Although the origin of the differences in the FTMS and ion mobility experiments is not resolved, we have postulated that differences may arise from the different timescales of the experiments (*13*). Exchange in the FTMS instrument occurs over seconds to minutes, whereas in a drift tube it requires only milliseconds. It is possible that exchange over longer timescales allows conformations to fluctuate, exposing regions that were protected, allowing extensive exchange. Similar mechanisms operate in solution-exchange processes. During the short timescales of the ion mobility experiment, conformations may not undergo substantial fluctuations. Thus, the drift tube experiment may provide what is effectively a snapshot of the most rapidly exchanging hydrogens. Current experiments in our laboratory are investigating H/D exchange over longer timescales.

Gas-phase protein folding. An important factor in folding of a protein in solution is the exclusion of solvent from regions that become the interior of the folded protein (the hydrophobic effect). Numerous recent experiments in the gas phase are directly testing the role of solvent in the folding of biomolecules (*17*). As previously discussed, the gas-phase conformations of proteins depend strongly on the charge state. As the charge state (and coulombic repulsion energy) increases, more open conformations are favored. A natural question to ask is, can a highly charged ion refold as protons are removed (*14, 15, 23–26*)?

We have explored this question for lysozyme—a 129-residue protein that contains four disulfide bonds in its native state—by first reducing the disulfide bonds of the protein in solution. ESI of the reduced protein yields only highly charged ions with elongated conformations (*15*). We then remove protons in the gas phase by allowing the highly protonated ions to undergo proton-transfer reactions with strong bases, such as butylamine, in a reaction cell before the drift tube. The mobilities of the lower charge-state ions that are formed during the proton-transfer reactions can be measured in order to examine changes in conformation that occur as protons are removed.

Figure 5 shows ion mobility distributions recorded for disulfide-intact and -reduced ions after being exposed to proton-transfer reagents in the gas phase. These data appear on a modified timescale (the drift time multiplied by the charge state), which normalizes differences in the effective drift field. With the disulfide bonds reduced, ESI favors high charge states (+10 to +18). All of these ions have conformations that are extremely elongated. ESI of the disulfide-intact solution favors lower charge states (+8 to +11) that are substantially more compact. At the +10 state, the effect of the disulfide bonds can be clearly noted; the disulfide-reduced ions have much more elongated conformations than the disulfide-intact ions. As protons are removed from the disulfide-reduced ions, the conformation contracts—a result consistent with coulombic repulsion energy decreasing (caused by the removal of a proton).

However, in addition to contraction of the elongated structures, new features in the ion mobility distributions are observed at shorter times. These must correspond to new, more compact conformations. The +9 state favors an elongated form, but a new peak (near 21 ms) near the favored conformer for the disulfide-intact +9 ion is also present. The +8 state of the disulfide-reduced lysozyme favors a conformer that is near in structure to that found for the disulfide-intact +8. A small shoulder observed in the distribution recorded for the reduced form has a drift

time identical to the main feature observed in the distribution for the +8 oxidized ion. The more compact forms of the lower charge states indicate that as charges are removed from the elongated forms of the highly charged ions, they fold up in the gas phase to form substantially more compact structures.

As an additional proton is removed, the +7 state of disulfide-reduced ion displays two features. The more compact of these features (from 13–17 ms) has a shape and position remarkably similar to the distribution recorded for the disulfide-intact ion. Removal of an additional proton yields the +6 state. Here, drift time distributions are superimposable for both forms of the ion.

The similar drift times (and cross sections) for the oxidized and reduced forms of the +6 to +8 states of lysozyme are extremely interesting. It is worth noting that this similarity does not require that the ions have the same conformations. However, it seems remarkable that when the elongated disulfide-reduced ions fold, the shapes and positions of some peaks in the drift time distributions are virtually indistinguishable from features observed in the data for the disulfide-intact ions. If one considers the idea that in addition to having identical cross sections, the conformations may also be similar, then it would appear that there are preferred folding pathways in the gas phase. In this case, the balance of columbic repulsion energy and attractive folding forces offers a means of trapping ions in partially folded states (*15*).

Outlook

The possibility of examining biomolecular conformation in the nearly ideal gas-phase environment is intriguing. This environment may provide a great deal of information to complement solution data. For example, factors that are important to biomolecular folding, such as electrostatic, intramolecular, and solvent-molecule interactions, can be examined in some detail.

The dynamics associated with unfolding and folding events appear accessible in the gas phase. These studies may have advantages compared with solution folding studies because of the balance between attractive folding forces and repulsive columbic interactions that can be controlled by varying the charge state of the gas-phase ion. By simultaneously examining the chemistry and shapes of conformations, information about the surfaces of in vacuo conformers may become clearer. The ability of ion mobility/MS methods to distinguish among different isomers and conformations may be tremendously valuable for characterizing oligosaccharides. The methods are becoming fast and sensitive; thus in the future they may find applications in characterizing other glycoconjugates. Finally, it is important to keep in mind that many of the ion mobility studies described here took place in the past year. This field is developing rapidly, and the outlook is promising.

We gratefully acknowledge support of this work by the National Science Foundation (Grant No. CHE-9625 199) and an ASMS research award generously provided by Finnigan MAT.

References

(1) Fenn, J. B.; Mann, M.; Meng, C. K.; Wong, S. F.; Whitehouse, C. M. *Science* **1989**, *246*, 64.
(2) Karas, M.; Hillenkamp, F. *Anal. Chem.* **1988**, *60*, 2299.
(3) von Helden, G.; Wyttenbach, T.; Bowers, M. T. *Science* **1995**, *267*, 1483.
(4) Wyttenbach, T.; von Helden, G.; Bowers, M. T. *J. Am. Chem. Soc.* **1996**, *118*, 8355.
(5) Clemmer, D. E.; Hudgins, R. R.; Jarrold, M. F. *J. Am. Chem. Soc.* **1995**, *117*, 10141.
(6) Clemmer, D. E.; Jarrold M. F. *J. Mass Spectrom.* **1997**, *32*, 577.
(7) St. Louis, R. H.; Hill, H. H. *Crit. Rev. Anal. Chem.* **1990**, *21*, 321.
(8) von Helden, G.; Hsu, M. T.; Kemper, P. R.; Bowers, M. T. *J. Chem. Phys.* **1991**, *95*, 3538.
(9) Jarrold, M. F.; Constant, V. A. *Phys. Rev. Lett.* **1992**, *67*, 2994.
(10) Bowers, M. T.; Kemper, P. R.; von Helden, G.; Van Koppen, P.A.M. *Science* **1993**, *260*, 1446.
(11) Clemmer, D. E.; Jarrold, M. F. *J. Am. Chem. Soc.* **1995**, *117*, 8841.
(12) Shelimov, K. B.; Clemmer, D. E.; Hudgins, R. R.; Jarrold, M. F. *J. Am. Chem. Soc.* **1997**, *119*, 2240.
(13) Valentine, S. J.; Clemmer, D. E. *J. Am. Chem. Soc.* **1997**, *119*, 3558.
(14) Shelimov, K. B.; Jarrold, M. F. *J. Am. Chem. Soc.* **1997**, *119*, 2987.
(15) Valentine, S. J.; Anderson, J.; Ellington, A. E.; Clemmer, D. E. *J. Phys. Chem. B* **1997**, *101*, 3891.
(16) Liu, Y.; Clemmer, D. E. *Anal. Chem.* **1997**, *69*, 2504.
(17) Woenckhaus, J.; Mao, Y.; Jarrold, M. F. *J. Phys. Chem. B* **1997**, *101*, 847.
(18) Valentine, S. J.; Counterman, A. E.; Clemmer, D. E. *J. Am. Soc. Mass Spectrom.* **1997**, *8*, 954.
(19) Covey, T. R.; Douglas, D. J. *J. Am. Soc. Mass Spectrom.* **1993**, *4*, 616.
(20) Cox, K. A.; Julian, R. K.; Cooks, R. G.; Kaiser, R. E. *J. Am. Soc. Mass Spectrom.* **1994**, *5*, 127.
(21) Collings, B. A.; Douglas, D. J. *J. Am. Chem. Soc.* **1996**, *118*, 4488.
(22) Winger, B. E.; Light-Wahl, J. J.; Rockwood, A. L.; Smith, R. D. *J. Am. Chem. Soc.* **1992**, *114*, 5897.
(23) McLafferty, F. W. et al. *Proc. Natl. Acad. Sci. U.S.A.* **1993**, *90*, 790.
(24) Wood, T. D.; Chorush, R. A.; Wampler III, F. M.; Little, D. P.; O'Connor, P. B.; McLafferty, F. W. *Proc. Natl. Acad. Sci. U.S.A.* **1995**, *92*, 2451.
(25) Williams, E. R. *J. Mass Spectrom.* **1996**, *31*, 831.
(26) Gross, D. S.; Schinier, P. D.; Rodriguez-Cruz, S. E.; Fagerquist, C. K.; Williams, E. R. *Proc. Natl. Acad. Sci. U.S.A.* **1996**, *93*, 3143.
(27) Sullivan, P. A.; Axelsson J.; Altmann, S.; Quist, A. P.; Sunqvist, B.U.R.; Riemann, C. T. *J. Am. Soc. Mass Spectrom.* **1996**, *7*, 329.
(28) Hoaglund, C. S.; Valentine, S. J.; Clemmer, D. E. *Anal. Chem.* **1997**, *69*, 4156.
(29) Mason, E. A.; McDaniel, E. W. *Transport Properties of Ions in Gases*; Wiley: New York, 1988.
(30) Mesleh, M. F.; Hunter, J. M.; Shvartsburg, A. A.; Schatz, G. C.; Jarrold, M. F. *J. Phys. Chem.* **1996**, *100*, 16082.
(31) Wyttenbach, T.; von Helden, G.; Batka Jr., J. J.; Douglas, C.; Bowers, M. T. *J. Am. Soc. Mass Spectrom.* **1997**, *8*, 275.
(32) Shvartsburg, A. A.; Jarrold, M. F. *Chem. Phys. Lett.* **1996**, *261*, 86.
(33) Wolynes, P. G. *Proc. Natl. Acad. Sci. U.S.A.* **1995**, *92*, 2426.
(34) Revercomb, H. E.; Mason, E. A. *Anal. Chem.* **1975**, *47*, 970.
(35) Dugourd, P.; Hudgins, R. R.; Clemmer, D. E; Jarrold, M. F. *Rev. Sci. Instrum.* **1997**, *68*, 1122.
(36) Quian, M. G.; Lubman, D. M. *Anal. Chem.* **1995**, *67*, 234 A.

David E. Clemmer is assistant professor at Indiana University. His research interests include characterizing the structures of macromolecules in the gas phase and protein folding. Yansheng Liu is currently employed by Kansas City Analytical. Stephen J. Valentine, Anne E. Counterman, and Cherokee S. Hoaglund are graduate students. Valentine's research interests include characterizing the structures of biomolecules in the gas phase using combined ion mobility and H/D exchange techniques. Counterman is working on characterizing the structures of biomolecular aggregates in the gas phase using ion mobility techniques. Hoaglund is currently interfacing ion mobility instruments with ion traps and time-of-flight mass spectrometers. Address correspondence regarding this article to Clemmer at Dept. of Chemistry, Indiana University, Bloomington, IN 47405.